

ORIGINAL ARTICLE

---

# Evaluation of Silver Ion-Releasing Scaffolds in a 3D Coculture System of MRSA and Human Adipose-Derived Stem Cells for Their Potential Use in Treatment or Prevention of Osteomyelitis

Mahsa Mohiti-Asli, PhD,<sup>1</sup> Casey Molina, BS,<sup>1</sup> Thamonwan Diteepeng, BS,<sup>2</sup> Behnam Pourdeyhimi, PhD,<sup>3</sup> and Elizabeth G. Lobo, PhD<sup>1,4</sup>

Bone infection, also called osteomyelitis, can result when bacteria invade a bone. Treatment of osteomyelitis usually requires surgical debridement and prolonged antimicrobial therapy. The rising incidence of infection with multidrug-resistant bacteria, in particular methicillin-resistant *staphylococcus aureus* (MRSA), however, limits the antimicrobial treatment options available. Silver is well known for its antimicrobial properties and is highly toxic to a wide range of microorganisms. We previously reported our development of biocompatible, biodegradable, nanofibrous scaffolds that released silver ions in a controlled manner. The objective of this study was to determine the efficacy of these scaffolds in treating or preventing osteomyelitis. To achieve this objective, antimicrobial efficacy was determined using a 3D coculture system of human adipose-derived stem cells (hASC) and MRSA. Human ASC were seeded on the scaffolds and induced to undergo osteogenic differentiation in both the absence and presence of MRSA. Our results indicated that the silver ion-releasing scaffolds not only inhibited biofilm formation, but also supported osteogenesis of hASC. Our findings suggest that these biocompatible, degradable, silver ion-releasing scaffolds can be used at an infection site to treat osteomyelitis and/or to coat bone implants as a preventative measure against infection postsurgery.

**Keywords:** nanofiber, antimicrobial, coculture, osteomyelitis

## Introduction

**O**STEOMYELITIS IS A DEBILITATING infectious disease characterized by severe inflammation and progressive bone destruction.<sup>1</sup> It can cause severe infection in bone, bone marrow, or surrounding soft tissue. Osteomyelitis usually occurs as a result of hematogenous spread of microorganisms to the bone from an indirect entry, such as contiguous infection or from an open wound caused by bone surgery or joint replacement.<sup>2</sup> The most common bacterium that has been isolated from more than half of the reported osteomyelitis cases is *Staphylococcus aureus*.<sup>1</sup> Treatment of bone infection is primarily through surgical debridement and removal of all necrotic tissue, followed by long-term admin-

istration of intravenous and oral antibiotics.<sup>3,4</sup> Typically, high doses of antibiotics are needed to achieve an effective therapeutic drug concentration in the bone. This can cause systemic toxicity.<sup>5</sup> Despite continuing advances in surgical procedures and use of antibiotics, up to 30% of treatments fail and patients with osteomyelitis develop chronic infections.<sup>6</sup> This could be due to avascularity of developing sequestra, inhibiting the ability of antibiotics and inflammatory cells to reach the infected site.<sup>1</sup> Alternative strategies are, therefore, critical to investigate.

Controlled antimicrobial release systems are new strategies to prevent and treat chronic osteomyelitis. Such systems enable administration of higher antimicrobial concentrations at the site of infection for prolonged duration without systemic

---

<sup>1</sup>Joint Department of Biomedical Engineering, University of North Carolina at Chapel Hill and North Carolina State University, Raleigh, North Carolina.

<sup>2</sup>Silpakorn University, Nakornpathom, Thailand.

<sup>3</sup>College of Textiles, North Carolina State University, Raleigh, North Carolina.

<sup>4</sup>College of Engineering, University of Missouri, Columbia, Missouri.

toxicity. Some systems have been developed for local delivery of different antibiotics to infected bone, predominantly implementing a biomaterial that can release antibiotics. Biomaterials used for this purpose usually consist of a porous scaffold containing an osteoconductive compound such as hydroxyapatite,<sup>7</sup> calcium phosphate,<sup>8</sup> and/or recombinant human bone morphogenetic protein-2.<sup>9</sup> The most common antibiotic used in such local delivery platforms is vancomycin. Previous investigators have shown that scaffolds doped with vancomycin can inhibit the growth of *staphylococcus aureus*.<sup>9–11</sup> However, due to the vast increase in multidrug-resistant *Staphylococcus aureus* strains, utilization of antibiotics is becoming increasingly unsuccessful.

Silver is a broad-spectrum biocide that is toxic to a wide range of microorganisms. Previous investigators have evaluated local delivery of silver to an infection site.<sup>12</sup> Studies evaluating scaffolds for bone tissue engineering applications in the presence of bacteria have predominantly focused on incorporation of silver nanoparticles in an osteoconductive scaffold. Marsich *et al.* added silver nanoparticles to an alginate/hydroxyapatite composite through an adsorption process.<sup>13</sup> Their *in vitro* analyses were carried out for 7 days and indicated that the release of silver did not inhibit the proliferation of osteoblasts. In another study, silver nanoparticles were added to chitosan/hydroxyapatite scaffolds through a reduction phenomenon using functional groups of chitosan.<sup>14</sup> Cytotoxicity analyses of the scaffolds after 24 h showed that the scaffolds were not toxic to rat osteoprogenitor cells or human osteosarcoma cells. Although the short-term cell culture analyses in these studies,<sup>13,14</sup> and other similar studies<sup>15,16</sup> showed no cytotoxicity associated with the release of silver nanoparticles, concerns remain about the long-term effects of silver nanoparticles on host mammalian cells.<sup>17</sup> Some studies have shown that the very small size of nanoparticles allows them to diffuse within the cellular plasma membrane and interfere with a variety of cellular mechanisms.<sup>18,19</sup> Thus, in recent years, the Food and Drug Administration (FDA) and others<sup>20–22</sup> have expressed concern about the use of silver nanoparticles.

Recently, we reported development and validation of scaffolds capable of releasing silver ions at a controlled rate without the use of silver nanoparticles.<sup>23</sup> The scaffolds are comprised of polylactic acid (PLA) nanofibers coated with a proprietary polymer containing silver nitrate (Silvadur ET; Dow Chemical Company). This nanofibrous delivery platform is biocompatible and biodegradable, eliminating the need for removal surgery. We previously showed that these scaffolds were effective in inhibiting growth of *Staphylococcus aureus*.<sup>23</sup> The goal of this study was to evaluate efficacy of these scaffolds against multidrug-resistant *Staphylococcus aureus* (MRSA) and potential utilization of these materials for bone tissue engineering and/or bone regeneration in an environment contaminated with MRSA.

To evaluate the potential use of these antimicrobial scaffolds for osteomyelitis and/or bone tissue engineering in infected wound sites, osteogenesis of human adipose-derived stem cells (hASC) seeded on these scaffolds was determined. To better mimic the osteomyelitis state *in vitro*, a coculture system of hASC and MRSA was developed by modifying a previously published coculture technique used for evaluation of wound dressings.<sup>24</sup> In particular, our system allows for simultaneous evaluation of the scaffolds' antimicrobial

properties, while also assessing their ability to support osteogenic differentiation of human stem cells. As opposed to previous studies, which evaluated antimicrobial and osteogenic differentiation analyses of their materials in separate cell culture experiments,<sup>15,16</sup> our system allows for *in vitro* analyses in an environment that includes interactions of human stem cells with MRSA bacteria in the same culture system. This newly modified coculture system also provides a platform for evaluation of other controlled release systems for their efficacy in addressing osteomyelitis. To our knowledge, this is the first study to evaluate a biomaterial for its ability to simultaneously promote osteogenic differentiation of human stem cells, while also exhibiting antimicrobial efficacy in a coculture system comprised of both hASC and MRSA.

## Materials and Methods

### Fabrication of antimicrobial scaffolds

PLA nanofibrous scaffolds were fabricated as previously described.<sup>23</sup> Briefly, PLA (MW: 70,000 g mol<sup>-1</sup>) was dissolved in chloroform and dimethylformamide (Sigma) at a ratio of 3:1 to create an 11% polymeric solution. The solution was stirred at 80°C for 4 h and then electrospun in a custom electrospinning system. The electrospun PLA nanofibers were immersed for 1 h in a diluted solution of Silvadur ET containing 31.25 µg/mL silver. Nanofibrous scaffolds were then dried under a fume hood for 24 h to form a thin antimicrobial coating. Coated scaffolds were cut into circles (1 cm diameter) and sterilized with ethylene oxide gas for 12 h.

### Culture of hASC

Human adipose tissue was obtained from a voluntary liposuction procedure performed on a 36-year-old Caucasian female in accordance with an approved IRB protocol (IRB-04-1622) at the University of North Carolina, Chapel Hill. hASC were isolated from the adipose tissue as previously reported by our laboratory.<sup>25,26</sup> Human ASC were expanded to passage 3 and maintained in complete growth medium (CGM) (alpha minimum essential medium [ $\alpha$ -MEM] [88%], fetal bovine serum [FBS, 10%], L-glutamine [1%], and penicillin/streptomycin [1%]) in 75-cm<sup>2</sup> tissue culture flasks until they reached 80% confluency (approximately 10 days). Human ASC were then trypsinized and suspended in a predetermined volume of CGM to achieve the concentration of 250,000 cells mL<sup>-1</sup>. Eighty microliters of the prepared cell suspension was added on top of each scaffold.

### Culture of MRSA

MRSA bacteria (ATCC<sup>®</sup> BAA-44<sup>™</sup>) were streaked for isolation on a soybean casein digest agar plate (Fisher Scientific). The agar plate was incubated (37°C, 5% CO<sub>2</sub>) overnight and then a single isolated MRSA colony was selected and used to inoculate 5 mL of Muller-Hinton (MH) broth (Difco Laboratories). After culture overnight, the bacterial concentration was determined by measurement of the optical density of the bacterial suspension using a UV-Vis spectrophotometer (BioMate3, Thermo Electron Corporation) at a wavelength of 600 nm. The bacterial concentration was then adjusted by serial dilution to acquire the concentrations utilized for the following experiments.

### Evaluation of antimicrobial efficacy of silver-releasing scaffolds against MRSA: AATCC 147 protocol

The standard AATCC 147 test, also known as the “parallel streak method,” was utilized to evaluate the antimicrobial efficacy of the silver-releasing scaffolds against MRSA. A  $1.5 \times 10^8$  CFU/mL (0.5 McFarland) suspension of MRSA bacteria in phosphate-buffered saline (PBS) was prepared and spread over each agar plate using a sterile swab to prepare bacterial lawns. Silver-releasing scaffolds (1.6 cm diameter) were placed in the center of the bacterial lawn and incubated overnight. Bactericidal activity was then visually assessed to determine the zone of inhibition around the scaffold to evaluate antimicrobial efficacy of the scaffolds against MRSA.

### Coculture system of hASC with MRSA

Osteogenic differentiation of hASC seeded on the antimicrobial scaffolds in the presence of MRSA was evaluated in a 3D coculture system using an adaptation of our previously published technique.<sup>24</sup> Briefly, antimicrobial scaffolds were seeded with hASC at a density of  $2 \times 10^4$  hASC per square centimeter. The cell-seeded scaffolds were placed into the separate wells of 24-well plates. One microliter of CGM without penicillin/streptomycin was pipetted into each well and the plates were incubated for 24 h. The CGM was then replaced with 1 mL osteogenic differentiation medium (ODM) (CGM without antibiotics and supplemented with  $5 \times 10^{-5}$   $\mu$ M ascorbic acid,  $0.1 \times 10^{-6}$  M dexamethasone, and  $10^{-2}$  M  $\beta$ -glycerophosphate) containing 10 CFU/mL MRSA bacteria. Scaffolds seeded with hASC and inoculated with MRSA were then incubated for 2 weeks. Daily, the medium was pipetted up and down several times, to ensure bacteria were well suspended in the medium, and one-half of the bacterial suspension was then taken out of the plates and replaced with fresh ODM.

Separate experiments with only hASC or MRSA bacteria were also performed to better interpret and elucidate the results of the coculture system. Pure PLA scaffolds (containing no silver) were used as controls for all experimental conditions.

### Monitoring MRSA growth in coculture system

For daily evaluation of the bacterial concentration, harvested bacterial suspensions were diluted multiple times, and spread on agar plates. Agar plates were incubated overnight to allow bacterial colonies to grow and become visible to the naked eye for counting.

### Monitoring osteogenic differentiation of hASC in a coculture system

Osteogenic differentiation of hASC seeded on the scaffolds was determined by quantification of total calcium accretion, a measure of mineral deposition, on days 7 and 14. Scaffolds were washed three times with  $1 \times$  PBS and calcium was solubilized by overnight immersion of scaffolds in 0.5 N hydrogen chloride (HCl). The supernatants were collected and assayed using the Calcium LiquiColor Kit (Stanbio Laboratory). To perform the assay, 10  $\mu$ L of supernatants were mixed with 200  $\mu$ L of assay reagent solution as per the manufacturer’s instructions for microplate analyses, and absorbance read at 550 nm using a microplate reader (TECAN GENios). Calcium chloride ( $\text{CaCl}_2$ ) was used to generate a standard curve as per the manufacturer’s instructions. The standard curve was used to determine sample calcium concentration. Calcium accretion data were normalized to total DNA using the DNA Hoechst fluorescence assay.

To measure the total DNA, scaffolds were washed at least three times with PBS to confirm that the bacteria were detached from the scaffolds. Samples were vortexed during the washing process to assist with the detachment of bacteria. To verify that all bacteria were washed out from the scaffolds, the PBS solution from the last wash was used for bacterial analysis to confirm no bacteria were present in the PBS from the last wash. Once this was confirmed, the amount of DNA in each nanofibrous scaffold was then measured with DNA-binding dye, Hoechst 33258, in microplate format after overnight digestion at 60°C in 2.5 U/mL papain in PBS with 5 mM ethylenediaminetetraacetic acid and 5 mM cysteine HCl (all reagents from Sigma). Fluorescence was measured at an excitation wavelength of 352 nm and emission wavelength of 461 nm on a microplate reader. A DNA standard curve was generated using DNA derived from calf thymus (Sigma) and DNA concentration was calculated as a function of fluorescence.

Calcium accretion was also visualized by staining calcium deposits using Alizarin Red S (Acros Organics). Scaffolds were harvested at 7 and 14 days and placed in 10% formalin for 30 min to fix cells adhered to the scaffolds. Cell-seeded scaffolds were then stained with 2% Alizarin Red S (pH 4.2) for 3 min and rinsed with deionized water three times to remove any unbound stain. Light microscopy images were captured with a Leica EZ 4D Digital Dissecting Scope.

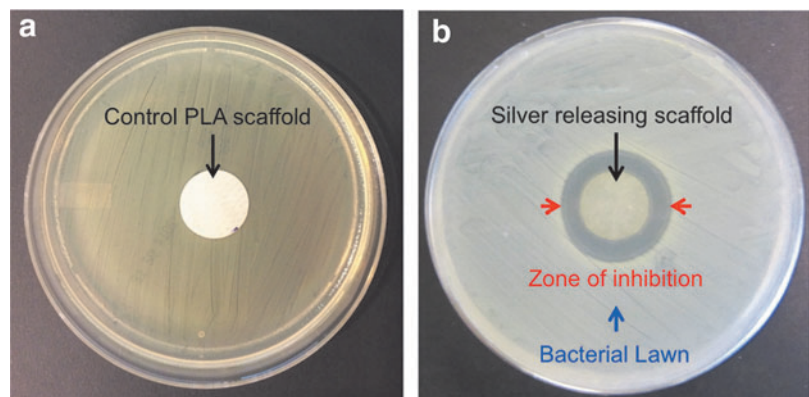


**FIG. 1.** Antimicrobial efficacy of control PLA scaffolds (a) and silver-releasing scaffolds (b) against MRSA bacteria as evaluated by the AATCC 147 test. MRSA, Methicillin-resistant *staphylococcus aureus*; PLA, polylactic acid. Color images available online at [www.liebertpub.com/tea](http://www.liebertpub.com/tea)

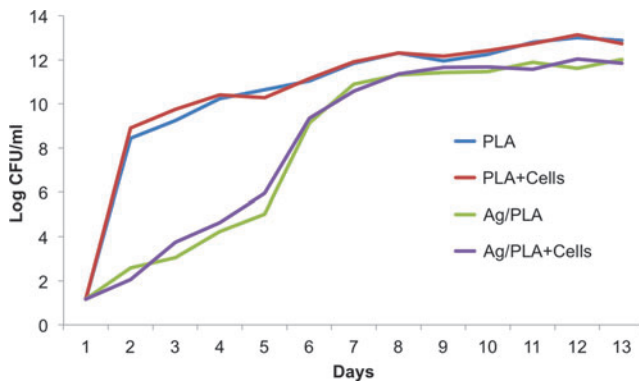


**FIG. 2.** Growth of MRSA bacteria over 2 weeks when cultured with acellular or hASC-seeded PLA and silver-releasing PLA (Ag/PLA) scaffolds. hASC, adipose-derived stem cell. Color images available online at [www.liebertpub.com/tea](http://www.liebertpub.com/tea)

### Microscopy analyses

Surface topography of the scaffolds was evaluated using scanning electron microscopy (SEM) (FESEM JEOL 6400 F) at 15 kV accelerating voltage. Nanofibrous scaffolds were fixed in 10% buffered formalin for 30 min then dehydrated in a graded series of increasing ethanol concentrations (50–100%). Dehydrated scaffolds were chemically dried by immersion in hexamethyldisilazane for 15 min then air dried overnight in a fume hood. Scaffolds were then sputter coated with gold to visualize surface morphology using SEM.

### Statistical analyses

All experiments were performed using at least three technical replicates. Statistical analyses were performed using SPSS 14.0. Data were analyzed using Duncan test with *p*-values less than 0.05 considered statistically significant.

## Results

### Evaluation of antimicrobial efficacy of silver-releasing scaffolds against MRSA—AATCC 147 protocol

After overnight incubation of the silver-releasing scaffolds on MRSA-inoculated agar plates, a clear zone of inhibition

was observed around the scaffolds confirming effectiveness of these materials against MRSA (Fig. 1).

### Monitoring MRSA growth in hASC/MRSA coculture system

Concentration of MRSA in cultures with control PLA (i.e., pure PLA with no silver) scaffolds, either acellular or seeded with hASC, increased rapidly by 8 log one day after culture (Fig. 2). Growth of MRSA in these cultures continued with a slower rate thereafter. Growth of MRSA in cultures with silver-releasing scaffolds was significantly decreased for the first 5 days. The bacterial concentration displayed the largest growth on day 6 and then continued the trend of increasing growth, although at a diminished rate (Fig. 2).

### Scanning electron microscopy analyses of scaffolds

Scanning electron microscopy revealed growth of MRSA over 2 weeks between the fibers of both control PLA and silver-releasing scaffolds (Fig. 3). The images showed formation of a biofilm, a dense layer of bacteria, on both cell-seeded and acellular PLA scaffolds (Fig. 3). However, although MRSA also grew in the silver-releasing scaffolds, no evidence of biofilm formation was observed on these scaffolds.

### Osteogenic differentiation of hASC in hASC/MRSA coculture system

To qualitatively assess cell-mediated calcium accretion, calcium deposition was visualized using Alizarin Red S on days 7 and 14 (Fig. 4). After 7 days of culture, mineralization occurred for all samples. On day 14, significant increases in mineralization were noted for all samples (Fig. 4).

Mineralization of hASC was quantified on days 7 and 14 for total calcium content in the scaffolds (Fig. 5). Mineralization of hASC seeded on silver-releasing scaffolds was not significantly different from that of hASC seeded on control PLA scaffolds after 7 and 14 days. With the introduction of MRSA to the cultures, mineralization of hASC seeded on control PLA scaffolds significantly decreased on day 7. In contrast, addition of MRSA to cultures with

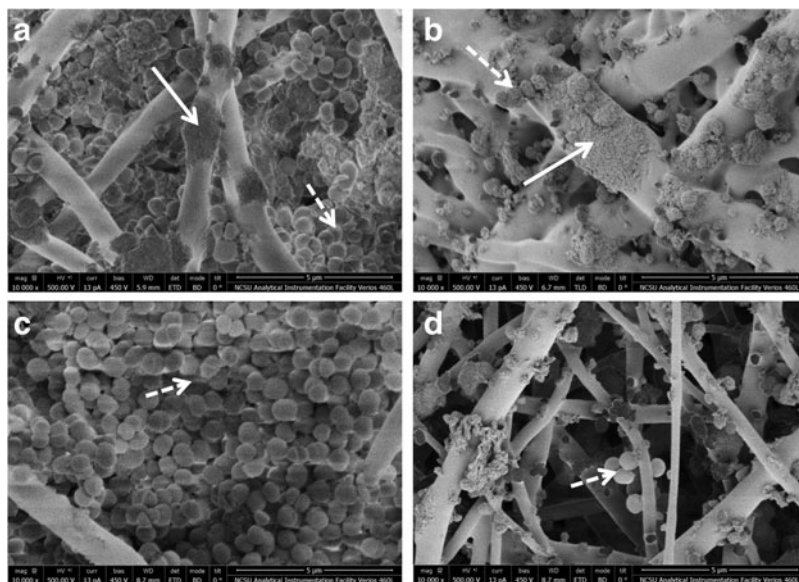
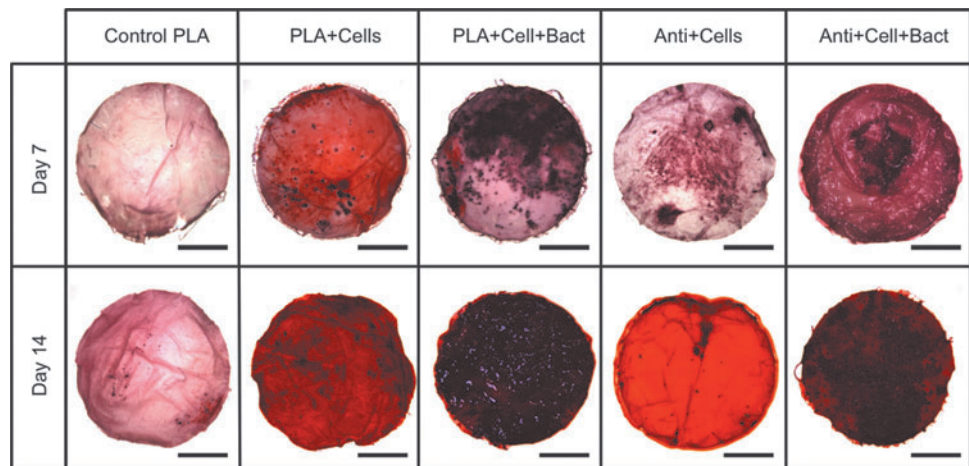


**FIG. 3.** Scanning electron microscopy photographs of scaffolds in MRSA suspensions after 2 weeks. (a) hASC-seeded control PLA (no silver) scaffolds, (b) hASC-seeded silver-releasing scaffolds, (c) acellular control PLA scaffolds (no hASC and no silver), and (d) acellular silver-releasing scaffolds. Solid arrows point to hASC and dashed arrows point to MRSA bacteria. Dense layer of MRSA bacteria, representing formation of biofilm, observed on both hASC-seeded and acellular PLA scaffolds, but not hASC-seeded or acellular silver-releasing scaffolds.

**FIG. 4.** Alizarin red staining of hASCs-seeded scaffolds in cultures with or without the presence of MRSA after 7 and 14 days. Scale bar is 3 mm. Control PLA=polylactic acid scaffolds without silver; Cells=hASC; Bact=MRSA; Anti=silver-releasing scaffold. Color images available online at [www.liebertpub.com/tea](http://www.liebertpub.com/tea)



silver-releasing scaffolds resulted in no significant difference in mineralization at this time point. By day 14, calcium accretion was significantly decreased for hASC on both scaffolds in the presence of MRSA relative to hASC osteogenic differentiation and calcium accretion in cultures without MRSA. However, cell-mediated calcium accretion was significantly higher for hASC seeded on antimicrobial scaffolds relative to those on control PLA scaffolds (Fig. 5).

## Discussion

In this study, the efficacy of a silver-releasing scaffold was evaluated for osteomyelitis using a 3D coculture of hASC and MRSA. We previously developed and evaluated similar scaffolds for skin tissue engineering applications.<sup>23</sup> We found in that study that a silver concentration of 31.25  $\mu\text{g}/\text{mL}$  in the coating solution allowed for enough silver ion release to inhibit the growth of *S. aureus* (methicillin-resistant *S. aureus* not evaluated in that study) without causing cytotoxicity to human skin cells.<sup>23</sup> The same silver concentration was incorporated in the scaffolds used for this study and their

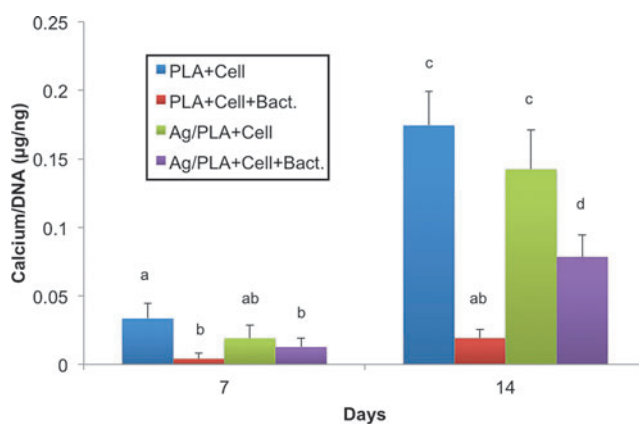


**FIG. 5.** Calcium accretion quantification of hASC (Cell) seeded on PLA and silver-releasing PLA (Ag/PLA) scaffolds and induced to undergo osteogenic differentiation in cultures with or without the presence of MRSA (Bact). Columns with different letters indicate significant difference ( $p < 0.05$ ). Color images available online at [www.liebertpub.com/tea](http://www.liebertpub.com/tea)

effectiveness against MRSA was evaluated. Our results confirmed that these scaffolds were capable of both inhibiting growth of and killing MRSA, a superbug of increasing threat to patients with osteomyelitis.

To evaluate the potential efficacy of these scaffolds for osteomyelitis, a 3D coculture system of hASC and MRSA was designed based on a modification of our previously published technique.<sup>24</sup> In this system, both osteogenesis of hASC and growth of MRSA were simultaneously evaluated. We found that the silver-releasing scaffolds were capable of significantly delaying the growth of MRSA (Fig. 2). Specifically, the bacterial growth rate was significantly slower for the first 5 days. Management of bacterial growth in the early stages of osteomyelitis is critical as it can decrease chances of developing chronic osteomyelitis. Although the bacterial growth in cultures with silver-releasing scaffolds was not fully inhibited, likely due to the high concentration of bacteria relative to the size of the scaffold used, the materials appeared to inhibit biofilm formation (Fig. 3). Formation of a biofilm allows for immune evasion and resistance to antimicrobial agents.<sup>27</sup> When such biofilms are formed on bones as occurs with osteomyelitis, the gold standard of care is to surgically remove the bone.<sup>1</sup>

It is essential to ensure that scaffolds used to deliver antimicrobial agents to the infected bone site do not cause cytotoxicity of human stem and bone cells and do not inhibit osteogenesis. Our coculture system allowed assessment of the antimicrobial efficacy of our scaffolds in an *in vitro* environment that resembles osteomyelitis. Both Alizarin Red staining and calcium deposition quantification results confirmed that the silver-releasing scaffolds allowed for continued osteogenesis of hASC on the antimicrobial scaffolds, an outcome that was not achieved using pure PLA scaffolds. Future studies could expand upon this work to evaluate release of inflammatory mediators, such as interleukin-1beta (IL-1 $\beta$ ), interleukin-6 (IL-6), interleukin-8 (IL-8) and/or tumor necrosis factor alpha (TNF- $\alpha$ ).

This is the first study to develop a 3D coculture system for evaluation of antimicrobial scaffolds for osteomyelitis. Our findings suggest the potential use of our silver-releasing scaffolds in treating bone infection, for bone tissue engineering in an infected wound site, and/or as a coating on bone implants to prevent osteomyelitis.

### Acknowledgments

This research was supported by NIH/CTSA 550KR71418 (EGL), NIH/CTSA 550KR61325 (EGL), NSF/CBET 1133427 (EGL), and a North Carolina Biotechnology Center Collaborative Funding Grant (EGL). The authors would like to acknowledge all the members of the Cell Mechanics Laboratory.

### Disclosure Statement

No competing financial interests exist.

### References

- Lew, D.P., and Waldvogel, F.A. Osteomyelitis. *Lancet* **364**, 369, 2004.
- Garzoni, C., and Kelley, W.L. Staphylococcus aureus: new evidence for intracellular persistence. *Trends Microbiol* **17**, 59, 2009.
- Waldvogel, F.A., Medoff, G., and Swartz, M.N. Osteomyelitis: a review of clinical features, therapeutic considerations and unusual aspects. *N Engl J Med* **282**, 198, 1970.
- Kahn, D.S., and Pritzker, K.P. The pathophysiology of bone infection. *Clin Orthop Relat Res* **96**, 12, 1973.
- Nandi, S.K., Mukherjee, P., Roy, S., Kundu, B., De, D.K., and Basu, D. Local antibiotic delivery systems for the treatment of osteomyelitis—A review. *Mater Sci Eng C* **29**, 2478, 2009.
- Conterno, L.O., and da Silva Filho, C.R. Antibiotics for treating chronic osteomyelitis in adults. *Cochrane Database Syst Rev* **3**, CD004439, 2009.
- Hess, U., Hill, S., Treccani, L., Streckbein, P., Heiss, C., and Rezwani, K. A mild one-pot process for synthesising hydroxyapatite/biomolecule bone scaffolds for sustained and controlled antibiotic release. *Biomed Mater* **10**, 015013, 2015.
- Zhang, Y., and Zhang, M. Calcium phosphate/chitosan composite scaffolds for controlled in vitro antibiotic drug release. *J Biomed Mater Res* **62**, 378, 2002.
- Doty, H.A., Leedy, M.R., Courtney, H.S., Haggard, W.O., and Bumgardner, J.D. Composite chitosan and calcium sulfate scaffold for dual delivery of vancomycin and recombinant human bone morphogenetic protein-2. *J Mater Sci Mater Med* **25**, 1449, 2014.
- Pacheco, H., Vedantham, K., Young, A., Marriott, I., and El-Ghannam, A. Tissue engineering scaffold for sequential release of vancomycin and rhBMP2 to treat bone infections. *J Biomed Mater Res Part A* **102**, 4213, 2014.
- Li, B., Brown, K.V., Wenke, J.C., and Guelcher, S.A. Sustained release of vancomycin from polyurethane scaffolds inhibits infection of bone wounds in a rat femoral segmental defect model. *J Controll Release* **145**, 221, 2010.
- Atiyeh, B.S., Costagliola, M., Hayek, S.N., and Dibo, S.A. Effect of silver on burn wound infection control and healing: review of the literature. *Burns* **33**, 139, 2007.
- Marsich, E., Bellomo, F., Turco, G., Travan, A., Donati, I., and Paoletti, S. Nano-composite scaffolds for bone tissue engineering containing silver nanoparticles: preparation, characterization and biological properties. *J Mater Sci Mater Med* **24**, 1799, 2013.
- Saravanan, S., Nethala, S., Pattnaik, S., Tripathi, A., Moorthi, A., and Selvamurugan, N. Preparation, characterization and antimicrobial activity of a bio-composite scaffold containing chitosan/nano-hydroxyapatite/nano-silver for bone tissue engineering. *Int J Biol Macromol* **49**, 188, 2011.
- Sun, C., Che, Y., and Lu, S. Preparation and application of collagen scaffold-encapsulated silver nanoparticles and bone morphogenetic protein 2 for enhancing the repair of infected bone. *Biotechnol Lett* **37**, 467, 2015.
- Zheng, Z., Yin, W., Zara, J.N., Li, W., Kwak, J., Mamidi, R., Lee, M., Siu, R.K., Ngo, R., and Wang, J. The use of BMP-2 coupled-Nanosilver-PLGA composite grafts to induce bone repair in grossly infected segmental defects. *Biomaterials* **31**, 9293, 2010.
- Bondarenko, O., Juganson, K., Ivask, A., Kasemets, K., Mortimer, M., and Kahru, A. Toxicity of Ag, CuO and ZnO nanoparticles to selected environmentally relevant test organisms and mammalian cells in vitro: a critical review. *Arch Toxicol* **87**, 1181, 2013.
- Samberg, M.E., Lobo, E.G., Oldenburg, S.J., and Monteiro-Riviere, N.A. Silver nanoparticles do not influence stem cell differentiation but cause minimal toxicity. *Nanomedicine* **7**, 1197, 2012.
- Arora, S., Jain, J., Rajwade, J.M., and Paknikar, K.M. Cellular responses induced by silver nanoparticles: in vitro studies. *Toxicol Lett* **179**, 93, 2008.
- Trickler, W.J., Lantz, S.M., Murdock, R.C., Schrand, A.M., Robinson, B.L., Newport, G.D., Schlager, J.J., Oldenburg, S.J., Paule, M.G., and Slikker, W. Silver nanoparticle induced blood-brain barrier inflammation and increased permeability in primary rat brain microvessel endothelial cells. *Toxicol Sci* **118**, 160, 2010.
- Ahamed, M., Alsali, M.S., and Siddiqui, M.K. Silver nanoparticle applications and human health. *Clin Chim Acta* **411**, 1841, 2010.
- Johnston, H.J., Hutchison, G., Christensen, F.M., Peters, S., Hankin, S., and Stone, V. A review of the in vivo and in vitro toxicity of silver and gold particulates: particle attributes and biological mechanisms responsible for the observed toxicity. *Critic Rev Toxicol* **40**, 328, 2010.
- Mohiti-Asli, M., Pourdeyhimi, B., and Lobo, E.G. Novel, silver-ion-releasing nanofibrous scaffolds exhibit excellent antibacterial efficacy without the use of silver nanoparticles. *Acta Biomater* **10**, 2096, 2013.
- Mohiti-Asli, M., Pourdeyhimi, B., and Lobo, E. Skin tissue engineering for the infected wound site: biodegradable PLA nanofibers and a novel approach for silver ion release evaluated in a 3D co-culture system of keratinocytes and *Staphylococcus aureus*. *Tissue Eng Part C* **20**, 790, 2014.
- Wall, M.E., Rachlin, A., Otey, C.A., and Lobo, E.G. Human adipose-derived adult stem cells upregulate palladin during osteogenesis and in response to cyclic tensile strain. *Am J Physiol Cell Physiol* **293**, C1532, 2007.
- Wall, M.E., Bernacki, S.H., and Lobo, E.G. Effects of serial passaging on the adipogenic and osteogenic differentiation potential of adipose-derived human mesenchymal stem cells. *Tissue Eng* **13**, 1291, 2007.
- Brady, R.A., Leid, J.G., Calhoun, J.H., Costerton, J.W., and Shirtliff, M.E. Osteomyelitis and the role of biofilms in chronic infection. *FEMS Immunol Med Microbiol* **52**, 13, 2008.

Address correspondence to:  
Elizabeth Lobo, PhD  
College of Engineering  
University of Missouri  
Columbia, MO 65211

E-mail: eglobo@missouri.edu

Received: February 15, 2016

Accepted: September 13, 2016

Online Publication Date: October 25, 2016